Reference: *Biol. Bull.* **195:** 5–11. (August, 1998)

Sickling of Anoxic Red Blood Cells in Fish

FERENC I. HÁROSI[1,*], IONE HUNT VON HERBING[2], AND JEFFREY R. VAN KEUREN[3]

[1] *Laboratory of Sensory Physiology, Marine Biological Laboratory, Woods Hole, Massachusetts 02543, and Department of Physiology, Boston University School of Medicine, Boston, Massachusetts 02118;* [2] *School of Marine Sciences, University of Maine, Orono, Maine 04469; and* [3] *Biology Department, Woods Hole Oceanographic Institution, Woods Hole, Massachusetts 02543*

The occurrence of the mutant hemoglobin Hb S in human red blood cells results in sickle cell anemia. This disease, including its genetic and molecular bases, has been extensively investigated and is well understood (1,2). The presence of deoxy-induced sickling of animal erythrocytes is largely unknown, however. We examined red blood cells (RBCs) from several fish species in vitro *under aerated and anoxic conditions. Our polarized light microscopic techniques were aimed at establishing correlations between erythrocyte morphology, state of oxygenation, spectral absorbance, linear dichroism, and linear birefringence. We found no fish with intracellular HbO_2 polymerization; but there were intraerythrocytic aggregations of deoxy Hb with a high degree of either molecular order or disorder. The ordered aggregates in the RBCs of Atlantic cod, haddock, and toadfish were remarkably similar in dichroic ratio magnitudes and birefringence to those in human RBCs that contain HbS. Therefore, fish hemoglobins appear to be good models of sickling disorders and polymerization-related phenomena. The consequences of sickling on animal health and fish aquaculture remain to be studied.*

Aggregates of hemoglobin in fish erythrocytes have been reported since 1865 (cited in ref. 3). Nevertheless, former studies have failed to establish causal relationships between Hb aggregation, the state of oxygenation, and the attendant optical properties of erythrocytes (4–6). As a chance microspectrophotometric observation, we discovered linearly dichroic absorption of light by Hb in larval fish erythrocytes. This linear dichroism—*i.e.*, the dependence of the absorption coefficient on polarization direction—was associated with abnormal RBC shape, or "sickling," the common term for this condition. The cells with the distorted morphology contained intracellular "bodies" with high concentrations of deoxyhemoglobin; for the sake of simplicity we call these bodies "erythrosomes."

Erythrosomes are therefore intraerythrocytic, anisotropic aggregates of polymerized deoxy Hb that become visible in the light microscope because the refractive index of Hb is higher than that of the surrounding medium. Erythrosomes exhibit linear dichroism as well as linear birefringence and occur in varied forms. In the RBCs of larval haddock and cod, for example, they may appear as V, U, or "banana"-shaped structures; but at other stages, or in different species, they may be shaped like needles or rods. The sickled fish erythrocytes encountered to date have always been associated with deoxy Hb, and not the oxygenated form. Indeed, the sickling that appeared was readily reversible by aeration; that is, the erythrosomes disappear and the affected cells resume their normal shape upon oxygenation. Moreover, repeated cycles of anoxia and normoxia cause concomitant cycles of intracellular hemoglobin aggregation and dispersion. In these characteristics, sickling in fish mimics sickling in man.

Our initial observations of sickling were made on 8- and 60-day-old larval haddock (*Melanogrammus aeglefinus*, family Gadidae) as well as on 118- and 125-day-old Atlantic cod (*Gadus morhua*, family Gadidae), all of which derived from stocks originating in the Bay of Fundy, Canada. Because we did not know whether sickling in fish is restricted to the developmental stages of particular species or is a more widespread phenomenon, we extended our investigation to wild-caught and cultured specimens of several species from four other geographical locations.

Received 25 February 1998; accepted 5 June 1998.

* To whom correspondence should be addressed. E-mail: fharosi@mbl.edu

Typical spectral behavior of larval Atlantic cod RBC is illustrated in Figure 1. Erythrocytes with undistorted shape yielded the expected absorption spectrum for HbO_2 as shown in panel a: the Soret (or γ) band peaks at 414 nm and is not dichroic (dichroic ratio of 1). This is consistent with the presence of a random ensemble of HbO_2 molecules (α- and β-band peaks are at 574 and 540 nm, respectively). In marked contrast, the Soret-band in panel b peaks at 430 nm and shows significant linear dichroism with a peak ratio of about 2. The latter is indicative of an orderly arrangement of the chromophores *in situ* (no α-band and shifted β peak to 554 nm); thus the cod Hb behaves like the human Hb S. RBCs of juvenile Atlantic cod (age, 227 and 272 days) obtained from the Narragansett Laboratory of the National Marine Fisheries Service (Rhode Island), also sickled extensively (92%–95% of all cells) under anoxic conditions. Therefore, RBC sickling in cod and haddock is limited neither to an isolated stock nor to a specific age group, but is present in both larval and juvenile stages.

Of the 12 fish species tested, however, only 4 species exhibited sickling under our experimental conditions. These were the two gadids (Atlantic cod and haddock), the toadfish (*Opsanus tau*, family Batrachoididae), and the tautog (*Tautoga onitis*, family Labridae). Because all vertebrate hemoglobins are intracellular heterotetramers of the type $\alpha_2\beta_2$ (except for those of the cyclostomes) (1), and because sickling is controlled by the molecular makeup of the Hb molecules (1, 2), variations in sickling among the species appear to be due to variations in the globins. Such variability is in keeping with known amino acid variations in the α and β chains for which a great variety of mutations have been uncovered (1). In addition to interspecies variations, intraspecies variations were observed between different life history stages in tautog, but not haddock. In haddock, sickling occurred in all stages; but in tautog, sickling was common in the larva, rare in the juvenile stage, and absent in the adult.

Sickling in wild-caught adult toadfish was distinctive for the large erythrosomes produced. Under normoxic conditions, adult toadfish RBCs appeared as flattened ovoids containing isotropic HbO_2 (Fig. 2a); but in a sealed enclosure under anoxic conditions, virtually every RBC with an undamaged cell membrane sickled. Examples are shown in Figure 2b–d. The empirical Soret-band dichroic ratios determined for 100 erythrosomes yielded values between 1.3 and 2.5, with the distribution peaking at 2. Similar results were obtained with cod and haddock, so the erythrosomes in these three species resemble human sickle cells, which have yielded similar dichroic (polarization) ratio distributions peaking at 2.1 (7, 8).

RBC sickling in 37-day-old larval tautog was quite different from that in the former three species. Here, the most common path of aggregation followed the rims of

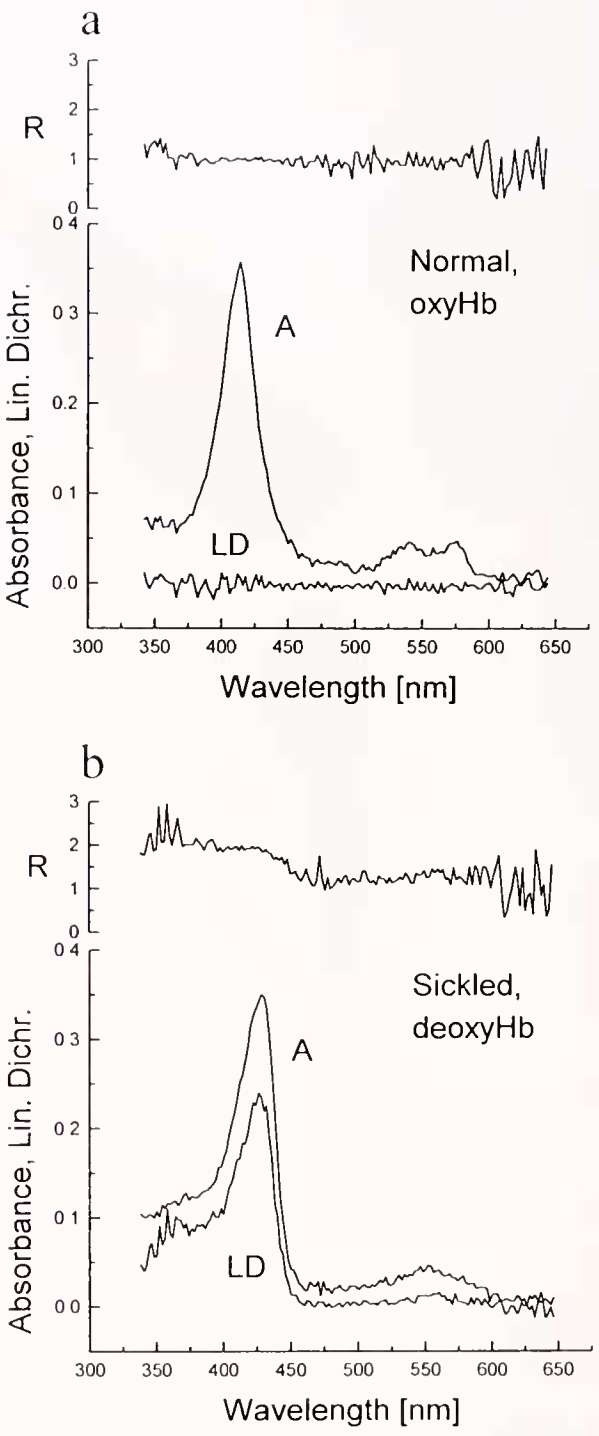

Figure 1. Larval Atlantic cod erythrocyte spectra under oxygenated (a) and deoxygenated (b) conditions: absorbance, A; linear dichroism, LD; and dichroic ratio, R. Absorbance was defined as $A = \log (I_r/I_s)$, where I_s and I_r are transmitted fluxes through sample and reference volumes of the preparation. Linear dichroism was proportional to transmission modulation by sample anisotropy, which was calibrated with an external polarizer to yield 1.0 full-scale value. Polarized absorbance components were determined (26, 27) parallel with erythrosome length for $A_{\parallel}$, and perpendicular to it for $A_{\perp}$. The dichroic ratio was computed as $R = A_{\perp}/A_{\parallel}$.

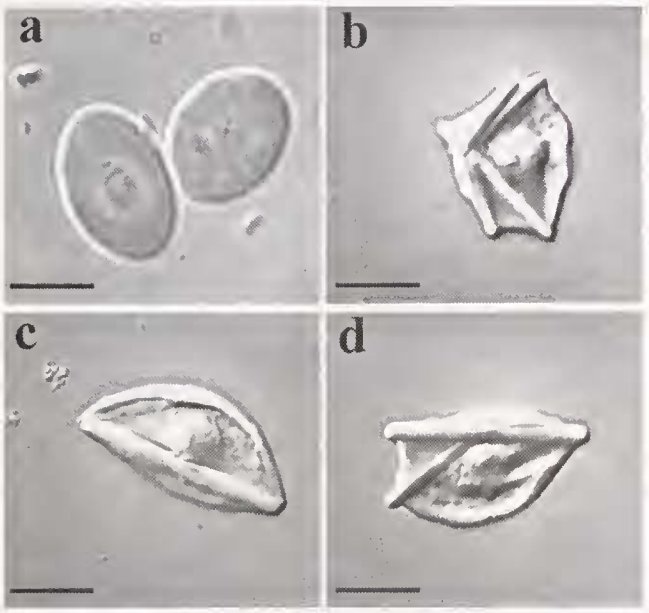

Figure 2. Photomicrographs of adult toadfish erythrocytes (nucleated, as all non-mammalian erythrocytes [9]) obtained with a Zeiss Axiophot 2 microscope in differential interference contrast mode (objective: Plan Apochromat, 63/1.4, oil immersion). (a) Normal cells containing HbO_2 with spectra like those of Fig. 1a. (b–d). Sickled cells under anoxic condition, each with spectra similar to those depicted in Fig. 1b. Scale bars, 10 μm.

the erythrocytes, usually forming elliptical and closed structures. The transverse-to-tangential dichroic ratio around the cells were nearly uniform, with $R \sim 1.5$. These results imply a flexible fibrous aggregation of Hb in which a degree of parallelism prevails. Unlike the toadfish case, tautog Hb polymerization seems to be too feeble to distort cells into "sickles"; rather it occurs along existing cellular features, such as hooplike microtubules (9).

Hemoglobin gelation in the summer flounder (*Paralichthys dentatus*, family Bothidae) is markedly different from that in either the toadfish or the tautog. Anoxic erythrocytes in the flounder may contain intraerythrocytic clumps without sickling. Aggregates of deoxy Hb in flounder remained isotropic and did not gel into regular structures. They exhibited no linear dichroism ($R \sim 1$). To distinguish isotropic from anisotropic aggregation, we regarded a cell to be sickled only when the Soret-band's linear dichroism was at least 10% above isotropic (*i.e.*, $R \geq 1.1$; see Table I).

Because a linearly dichroic sample should also have anisotropic polarizability, sickle cells would be expected to exhibit linear birefringence as well. Indeed, this has been observed (10) and measured (3) for human sickle cells. We found fish erythrosomes to be also birefringent. Figure 3a illustrates how toadfish erythrosomes may "light up" between crossed polarizers in various colorations depending on their orientation with respect to the polarizer's passing direction; they are the darkest at 0° and 90°, and brightest near 45° and 135°.

Retardance and absorbance spectra obtained from a typical toadfish erythrosome are depicted in Figure 3b. The retardance spectrum shows two peaks, one at 445–450 nm and the other at 585–590 nm; these peaks correspond to the longwave half-maxima of the γ and β-bands (with peaks at 430 and 556 nm, respectively). Although the latter behavior is consistent with *anomalous dispersion* (11,12), we currently lack a quantitative interpretation. The theory of anomalous dispersion describes variations in the relationship between refractive index and wavelength through regions of strong absorption: the index first declines with increasing wavelength, and then sharply rises before declining again to a higher plateau on the longwave side of an absorption band. The presence of the erythrosome's linear dichroism complicates matters. Here, the stronger absorption coincides with the slow direction of retardance, and the weaker absorption with the fast direction. Therefore, the two principal refractive indices undergo unequal dispersion and thus yield an "anomalous retardance." Whereas we expected erythrosomes to have *two intrinsic birefringent components*, one due to the heme groups and the other to the globin chains, their further delineation does not appear possible at present. Based on multiple determinations of retardance shown in Figure 3b (and assuming that the width of the erythrosome equals its thickness), the average *specific* retardance ($n = 16$) was in the range of 8.4 ± 1.4 nm/μm (450 nm) to 2.7 ± 0.6 nm/μm (540 nm). Thus, the average difference in the principal refractive indices, $|n_e - n_o|$, was variable in the visible spectrum between $2.7–8.4 \times 10^{-3}$. This range of values is to be compared with that of crystalline quartz, where the difference between the principal refractive indices is 9×10^{-3}. The explanation for erythrosome hues also follows from Figure 3b. Since light transmission of an erythrosome between crossed polarizers is proportional to retardance at each wavelength, and because peak retardance occurs around 450 nm, the transmitted flux should cause blue visual sensation at white illumination. If, on the other hand, retardance is also elevated for longer wavelengths (expected for thicker erythrosomes), increased transmission would result throughout the spectrum, yielding desaturated shades of blue.

The principal axes of birefringence were directly observable in polarized light by sample rotation. For toadfish erythrosomes, these correspond to their short and long dimensions, as can be seen in Figure 3a. However, a compensator is also needed if the slow direction is to be distinguished from the fast. To accomplish this, we used the Pol-Scope (13, 14), which is equipped with an automatic compensator. Figure 3c depicts brightness-encoded retardance images of several anoxic toadfish erythrocytes,

Table I

Fish erythrocyte properties: absorbance maxima and sickling

Species	Stage	OxyHb λ_{max} [nm]				DeoxyHb λ_{max} [nm]			
		γ	β	α	Sickling	γ	β	α	Sickling (%)*
Atlantic cod (*Gadus morhua*)	Larval	414	540	574	—	430	554	—	+ (~100)
	Juven.	414	540	574	—	430	554	—	+ (~95)
Haddock (*Melanogrammus aeglefinus*)	Larval	†	†	†	†	430	556	—	+ (~100)
	Juven.	414	540	575	—	430	556	—	+ (95)
	Adult	414	542	575	—	430	556	—	+ (91)
Toadfish (*Opsanus tau*)	Adult	414	540	576	—	430	556	—	+ (99)
Tautog (*Tautoga onitis*)	Larval	414	540	575	—	430	556	—	+ (~90)
	Juven.	414	542	576	—	430	556	—	+ (~1)
	Adult	414	542	576	—	430	556	—	—
Summer flounder (*Paralichthys dentatus*)	Juven.	414	542	576	—	430	560	—	—
Killifish (*Fundulus heteroclitus*)	Juven.	414	544	575	—	430	556	—	—
Sheepshead minnow (*Cyprinodon variegatus*)	Juven.	415	540	578	—	428	560	—	—
Blueback herring (*Alosa aestevalis*)	Juven.	414	539	575	—	430	555	—	—
Atlantic silverside (*Menidia menidia*)	Juven.	415	540	576	—	430	560	—	—
Smooth dogfish (*Mustelus canis*)	Adult	414	544	575	—	430	556	—	—
Little skate (*Raja erinacea*)	Adult	413	538	576	—	429	555	—	—
Common white sucker (*Catostomus commersoni*)	Adult	414	540	576	—	430	555	—	—

* In this column, + indicates the occurrence of optically anisotropic intraerythrocytic aggregates; ~ percentage was obtained by visual inspection of cell morphology; other fractions were based on measurable Soret-band linear dichroism ($R \geq 1.1$). The numeric values we regard only as approximate indicators of sickling, because polymerization is reversibly dependent on subtle variations in environmental conditions. Factors promoting sickling were anoxic conditions, low pH (6.9) and elevated temperature (29°C), analogous to those reported previously for Hb S.

† Unavailable data.

revealing bundles of linear molecular aggregation. Another cell from the same preparation is shown in Figure 3d, where an erythrosome retardance image with superimposed black lines indicates local slow axis direction: this direction is approximately transverse to the long dimension of the erythrosome. The line scans of erythrosome retardance are consistent with a model of fibrous molecular order which, taken together with the slow direction of retardation and coincident strong absorption, is in harmony with the presence of bundles of polymerized hemoglobin molecules with their planar porphyrin groups oriented nearly perpendicular to the length of the aggregation. These features have also been found in normal human reduced-hemoglobin crystals and in sickle cells from anemia patients (3).

Our polarized light microscopic observations are complementary to the structural information provided by electron microscopy. Thomas (15) used the latter technique on red cells of cod (*Gadus callarias*) and reported a paracrystalline organization for hemoglobin in erythrocytes. For atomic-scale comparison of fish hemoglobins with Hb S, it will be necessary to combine data from several techniques, as has been done for the various forms of human hemoglobin, including refined methods in electron microscopy (16), X-ray crystallography (17), and analyses of globin mutations based on amino acid sequence information (18).

The current investigation notwithstanding, we can only speculate how widespread sickling is among the nearly 20,000 extant fish species. But given the richly varied environments that fishes inhabit, a great variability in fish hemoglobins is probable. Also probable is that the evolution of fish hemoglobins has responded to various environmental stresses in many species. Thus, we anticipate fish hemoglobins to emerge as a rich resource for genetic, evolutionary, molecular, and pathophysiological studies. The variety of sickling hemoglobins may lead to new model systems, not only for a human disease, but also for studies of fundamental importance such as polymerization, force generation (19), and the identification of molecular contacts that make paracrystal formation possible.

The phenomenon of sickling may also have practical relevance to marine fish aquaculture. Fish in culture are often under heightened stress (*e.g.*, insufficient oxygenation, high bacterial load, and low pH), and they are consequently prone to infections and high mortality rates. Because a propensity for sickling could increase mortali-

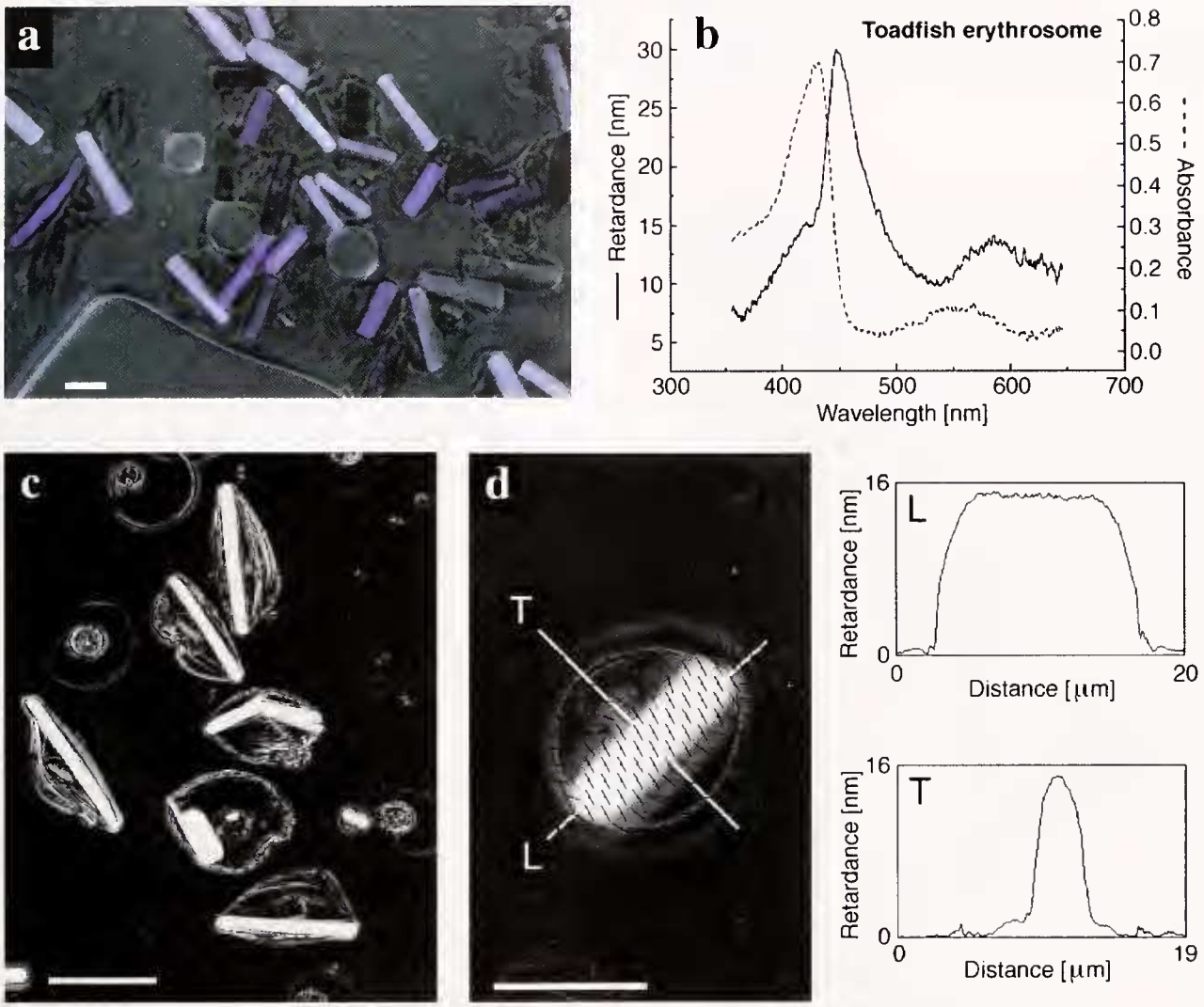

Figure 3. Toadfish erythrocytes. (a) Unstained, anoxic preparation between crossed polarizers at white light illumination (photographed in a Zeiss Axiophot 2 microscope on Kodak Ektachrome 160T film). (b) Retardance (solid) and absorbance (dashed) spectra of an isolated erythrosome (3.6 × 9 μm). (c) Retardance images from sickled and ghost cells measured at 546 nm with the Pol-Scope (13,14). The retardance for each picture element (pixel) was encoded in gray between 0 (black) and 16 nm (white). (d) Another Pol-Scope image of retardance with two line scans (inserts): longitudinal (L) and transverse (T) to the erythrosome. Scale bars, 10 μm.

ties, the molecular characterization of sickling hemoglobins in fishes and their attendant physiological manifestations are of paramount importance. The phenomenon is also relevant to restocking programs aimed at reestablishing dwindling groundfish populations.

Summary

Sickling in fish red blood cells is described, and the phenomenon is shown to occur in several species. By correlating the morphology of RBC with spectral absorption of Hb *in situ*, sickling is associated with the presence of deoxyhemoglobin. The polymerization of deoxy Hb is inferred from optical anisotropies measured in single cells. The magnitude of linear dichroism and the nature of linear birefringence detected in fish "erythrosomes" show close kinship to the corresponding properties determined previously from human sickle cells and hemoglobin crystals. The range of oxygen tension for sickling has not been determined and, therefore, we do not know whether it is within physiological limits. Also unknown is whether sickling in fish is pathological or, perhaps, reflective of a physiological condition with as yet obscure significance. In either case, however, further investiga-

tions promise to provide new insights into the requisite conditions that produce intracellular hemoglobin polymerization.

Methods

Sample preparation. Experiments were conducted at room temperature (20°–23°C). Our primary buffer (marine teleost Ringer's solution) contained (in m*M*): NaCl 140, KCl 2.5, $CaCl_2$ 1.5, $MgSO_4$ 1, NaH_2PO_4 0.5, $NaHCO_3$ 0.5, and HEPES 10, adjusted to pH 7.3 with NaOH. This was used (air-saturated) in about 10-fold excess to dilute whole blood for oxygenated preparations. Samples for microscopy were prepared in between two No. 1½ cover glasses sealed around the edge with a molten mixture of paraffin and Vaseline. The usual procedure was to place 3 μl of blood on a thoroughly cleaned (20, 21) microscope cover glass, either with or without a poly-L-lysine (P-1274, Sigma) coating (22, 23), add and mix 15–30 μl of desired buffer, cover, blot, and seal. Anoxic preparations were obtained in one of four ways: (1) By letting metabolically active blood cells deplete O_2. The effectiveness of this method is variable; for extensive sickling to occur, it may take from a few hours to 2–3 days. (2) By mounting erythrocytes and metabolically active retinal cells together in a sealed preparation, where complete deoxygenation may take only 30–120 min. This was the condition under which we first observed sickling. (3) By using N_2-purged dithionite solution (from 100 m*M* $Na_2S_2O_4$ stock) (24) and N_2-purged buffer (1:1) in preparing blood samples. (4) By the use of a calcium-free buffer (marine teleost Ringer without added calcium, containing 1 m*M* EGTA, at pH 6.9, and purged with N_2 for 1 h) and blood stored under light mineral oil (Paraffin, Fisher Scientific). The purpose of the oil is to keep the blood airtight, as previously reported (10). Additionally, we found that the oil prevents clotting for long periods (tested up to 8 weeks for toadfish blood); the latter method was found most effective in producing large, well-aligned erythrosomes.

Determination of absorbance and linear dichroism. We used the dichroic microspectrophotometer (25–27) with a measuring beam cross section of about 0.6 × 2 μm on cells in optical isolation. This instrument is a single-beam, phase-modulated, polarized light microscope equipped with automatic, wavelength-scanning and recording photometry. Glycerin immersion-type microscope objectives were used for both condensor (32×/0.4 Ultrafluar, Zeiss) and objective (100×/1.3 UV-F100, Nikon). Visualization was implemented with infrared light and a video camera system with tape recording.

Linear birefringence determination. The laboratory instrument was built around a modified Axiovert 10 (Zeiss) microscope utilizing quartz components and fiberoptic links between a 150-W xenon light source (Oriel Corp.) and a spectrograph-detector combination. Its adjustable cross section microbeam (about 1.5 × 4 μm) was passed through a rotatable polarizer (Glan-Thompson type); the condensor (32×/0.4 Ultrafluar, Zeiss); the preparation affixed to a rotatable, sliding stage; the objective (100×/1.2 Ultrafluar, Zeiss); and a slidable analyzer (HN38S, Meadowlark Optics). The transmitted light was collected and focused on the entrance slit of a spectrograph (MonoSpec 18, Jarrell Ash), which in turn dispersed it over an intensified diode array detector (Model 1455B, EG&G PARC). Electronic scanning of the latter provided records of spectral responses in the range of 350–650 nm. This instrument was also capable of determining absorbance and linear dichroism from static transmission measurements taken at appropriate sample orientations and polarizer settings. For the determination of linear birefringence, the preparation was positioned between crossed polarizers with the sample's principal (''slow'' and ''fast'') axes oriented at ±45° to the direction of polarization. The basis for signal processing was provided by the formula $I(\lambda) = I_p(\lambda)\{\sin^2[\Gamma(\lambda)/2] + 1/EF\}$, where $I(\lambda)$ is the transmitted flux at sample retardance of $\Gamma(\lambda)$ radians, $I_p(\lambda)$ the flux through the system for polarizer and analyzer axes set parallel [with $\Gamma(\lambda) = 0$], and EF is the extinction factor defined as $EF = I_p(\lambda)/I_c(\lambda)$ with $I_c(\lambda)$ being the transmitted flux for crossed polarizers (28). It followed from the foregoing that $\sin^2[\Gamma(\lambda)/2] = [I(\lambda) - I_c(\lambda)]/I_p(\lambda)$, wherefrom the retardance (in nm) at wavelength λ (nm) could be obtained as $\Gamma(\lambda) \approx \{[I(\lambda) - I_c(\lambda)]/I_p(\lambda)\}^{1/2}\,\lambda/\pi$ (assuming equality between the sine of small angles and their values in radians). The latter relationship was implemented on data sets from spectral scans of $I(\lambda)$, $I_c(\lambda)$ and $I_p(\lambda)$ by software operations using ORIGIN (Microcal Software). Birefringence is linked to retardance by the optical path difference in the sample between the fast and slow waves propagating through thickness d, $\Gamma(\lambda) = |n_e - n_o|d$, where n_e and n_o are the refractive indices along the two principal directions. The instrument's retardance determinations were tested on mica flakes as microscopic targets; the retardance and azimuth of the targets were previously measured (at 546 nm) in the Pol-Scope (13, 14). Good agreement was found between results of the two instruments for the retardance range used in this work.

Acknowledgments

The authors are grateful to D. Martin-Robichaud (St. Andrew's Biological Station, Department of Fisheries and Oceans, St. Andrew, N.B., Canada) for adult haddock blood; to L. Kling (Aquaculture Research Center, University of Maine) for providing cod and haddock larval and juvenile specimens; to L. J. Buckley and J. Allen (NOAA/

NMFS/NEFSC—Narragansett Laboratory, Rhode Island) for juvenile cod specimens; to G. Klein MacPhee (Graduate School of Oceanography, University of Rhode Island) for tautog and flounder specimens; to D. Perry, J. Hughes, and S. Burgh (NOAA/NMFS—Milford, Connecticut) for adult tautog blood; and to several colleagues at the Marine Biological Laboratory for supplying blood samples from various other organisms. We also thank R. Oldenbourg and K. Katoh for discussions and assistance with the Pol-Scope measurements, R. L. Nagel for advice, and I. Novales Flamarique for help with some experiments. Supported by grants from the US Public Health Service (EY04876 to F.I.H.), from Sea Grant development funds (to I.H.v.H.) and from the National Science Foundation (OCE 931-3680 to J.R.V.K.).

Literature Cited

1. **Bunn, H. F., and B. G. Forget. 1986.** *Hemoglobin: Molecular, Genetic and Clinical Aspects.* Saunders, Philadelphia.
2. **Eaton, W. A., and J. Hofrichter. 1987.** Hemoglobin S gelation and sickle cell disease. *Blood* **70:** 1245–1266.
3. **Perutz, M. F., and J. M. Mitchinson. 1950.** State of haemoglobin in sickle-cell anaemia. *Nature* **166:** 677–679.
4. **Yoffey, J. M. 1929.** A contribution to the comparative histology and physiology of the spleen, with reference chiefly to its cellular constituents. I. In fishes. *J. Anat.* **63:** 314–344.
5. **Dawson, A. B. 1932.** Intracellular crystallization of hemoglobin in the erythrocytes of the northern pipefish, *Syngnathus fuscus*. *Biol. Bull.* **63:** 492–495.
6. **Hansen, V. K., and K. G. Wingstrand. 1960.** Further studies on the non-nucleated erythrocytes of *Maurolicus Mülleri*, and comparisons with the blood cells of related fishes. Pp. 1–15 in *Dana-Report No. 54*, A. F. Host, Copenhagen.
7. **Hofrichter, J., D. G. Hendricker, and W. A. Eaton. 1973.** Structure of hemoglobin S fibers: optical determination of the molecular orientation in sickled erythrocytes. *Proc. Natl. Acad. Sci. USA* **70:** 3604–3608.
8. **Eaton, W. A., and J. Hofrichter. 1981.** Polarized absorption and linear dichroism spectroscopy of hemoglobin. Pp. 175–261 in *Methods in Enzymology*, Vol. 76, *Hemoglobins*. E. Antonini, L. Rossi-Bernardi, and E. Chiancone, eds. Academic Press, New York.
9. **Cohen, W. D. 1991.** The cytoskeletal system of nucleated erythrocytes. *Int. Rev. Cytol.* **130:** 37–84.
10. **Sherman, I. J. 1940.** The sickling phenomenon, with special reference to the differentiation of sickle cell anemia from sickle cell trait. *Bull. Johns Hopkins Hosp.* **67:** 309–324.
11. **Jenkins, F. A., and H. E. White. 1957.** *Fundamentals of Optics.* McGraw-Hill, New York.
12. **Born, M., and E. Wolf. 1975.** *Principles of Optics.* Pergamon Press, Oxford.
13. **Oldenbourg, R., and G. Mei. 1995.** New polarized light microscope with precision universal compensator. *J. Microsc.* **180:** 140–147.
14. **Oldenbourg, R. 1996.** A new view on polarization microscopy. *Nature* **381:** 811–812.
15. **Thomas, N. W. 1971.** The form of haemoglobin in the erythrocytes of the cod, *Gadus callarias*. *J. Cell Sci.* **8:** 407–412.
16. **Crepeau, R. H., and S. J. Edelstein. 1984.** Polarity of the 14-strand fibers of sickle cell hemoglobin determined by cross-correlation methods. *Ultramicroscopy* **13:** 11–18.
17. **Padlan, E. A., and W. E. Love. 1985.** Refined crystal structure of deoxyhemoglobin S. I. Restrained least-squares refinement at 3.0-Å resolution. *J. Biol. Chem.* **260:** 8272–8279.
18. **Nagel, R. L., *et al.* 1980.** β-Chain contact sites in the haemoglobin S polymer. *Nature* **283:** 832–834.
19. **Inoué, S. 1997.** The role of microtubule assembly dynamics in mitotic force generation and functional organization of living cells. *J. Struct. Biol.* **118:** 87–93.
20. **Inoué, S. 1986.** *Video Microscopy.* Plenum Press, New York.
21. **Fuseler, J. W. 1975.** Mitosis in *Tilia americana* endosperm. *J. Cell Biol.* **64:** 159–171.
22. **Mazia, D., G. Schatten, and W. Sale. 1975.** Adhesion of cells to surfaces coated with polylysine. *J. Cell Biol.* **66:** 198–200.
23. **Burr, A. H., and F. I. Hárosi. 1985.** Naturally crystalline hemoglobin of the nematode *Mermis nigrescens*. An *in situ* microspectrophotometric study of chemical properties and dichroism. *Biophys. J.* **47:** 527–536.
24. **Nagel, R. L., and H. Chang. 1981.** Methods for the study of sickling and hemoglobin S gelation. Pp. 760–792 in *Methods in Enzymology*, Vol. 76, *Hemoglobins*. E. Antonini, L. Rossi-Bernardi, and E. Chiancone, eds. Academic Press, New York.
25. **Hárosi, F. I., and E. F. MacNichol, Jr. 1974.** Dichroic Microspectrophotometer: a computer assisted, rapid, wavelength-scanning photometer for measuring linear dichroism in single cells. *J. Opt. Soc. Am.* **64:** 903–918.
26. **Hárosi, F. I. 1982.** Recent results from single-cell microspectrophotometry: cone pigments in frog, fish and monkey. *Color Res. Applic.* **7** (No. 2, Part 2): 135–141.
27. **Hárosi, F. I. 1987.** Cynomolgus and rhesus monkey visual pigments: application of Fourier transform smoothing and statistical techniques to the determination of spectral parameters. *J. Gen. Physiol.* **89:** 717–743.
28. **Inoué, S., and R. Oldenbourg. 1995.** Microscopes. Pp. 17.1–17.52 in *Handbook of Optics*, Vol. II, 2nd ed. M. Bass, ed. McGraw-Hill, New York.